Cholesterol sulfate and calcium affect stratum corneum lipid organization over a wide temperature range

J. A. Bouwstra,[1,*] G. S. Gooris,[*] F. E. R. Dubbelaar,[*] and M. Ponec[†]

Leiden/Amsterdam Center for Drug Research,* Gorlaeus Laboratories, Leiden University, P.O. Box 9502, 2300 RA Leiden, The Netherlands, and Department of Dermatology,† Leiden University Medical Center, Leiden, The Netherlands

Abstract **The main diffusion barrier for drugs penetrating through the skin is located in the intercellular lipid matrix in the upper layer of the skin, the stratum corneum (SC). The main lipid classes in the SC are ceramides (CER), free fatty acids (FFA) and cholesterol (CHOL). The lipids in SC are organized into two lamellar phases with periodicities of approximately 13 and 6 nm, respectively. Similar lipid organization has been found with equimolar CHOL:CER:FFA mixtures in SAXD studies performed at room temperature. However, one may conclude that the phase behavior of the mixtures is similar to that in SC only when the lipid organization of the lipid mixtures resembles that in SC over a wide temperature range. Therefore, in the present study, the organization of the lipid mixtures has been studied in a temperature range between 20° and 95°C. From these experiments it appeared that at elevated temperatures in equimolar CHOL:CER:FFA mixtures a new prominent 4.3 nm phase is formed between 35–55°C, which is absent or only weakly formed in intact human and pig SC, respectively. As it has been suggested that gradients of pH and cholesterol sulfate exist in the SC and that Ca^{2+} is present only in the lowest SC layers, the effect of pH, cholesterol sulfate, and Ca^{2+} on the lipid phase behavior has been investigated with lipid mixtures. Both an increase in pH from 5 (pH at the skin surface) to 7.4 (pH at the SC–stratum granulosum interface) and the presence of cholesterol sulfate promote the formation of the 13 nm lamellar phase. Furthermore, cholesterol sulfate reduces the amount of CHOL that is present in crystalline domains, causes a shift in the formation of the 4.3 nm phase to higher temperatures, and makes this phase less prominent at higher temperatures. The finding that Ca^{2+} counteracts the effects of cholesterol sulfate indicates the importance of a proper balance of minor SC components for appropriate SC lipid organization. In addition, when the findings are extrapolated to the in vivo situation, it seems that cholesterol sulfate is required to dissolve cholesterol in the lamellar phases and to stabilize SC lipid organization. Therefore, a drop in cholesterol sulfate content in the superficial layers of the SC is expected to destabilize the lipid lamellar phases, which might facilitate the desquamation process.**—Bouwstra, J. A., G. S. Gooris, F. E. R. Dubbelaar, and M. Ponec. **Cholesterol sulfate and calcium affect stratum corneum lipid organization over a wide temperature range.** ***J. Lipid Res.*** **1999.** 40: **2303–2312.**

Supplementary key words stratum corneum • ceramides • phase behavior • X-ray diffraction

One of the main functions of the skin is to act as a barrier for undesired exogenous substances. However, for topical application of drugs, this barrier forms the main problem. The skin barrier is located in the upper layer of the skin, the stratum corneum (SC) that is composed of keratin-rich cells surrounded by hydrophobic crystalline lipid lamellar domains. It has frequently been suggested that SC lipids play a dominant role in proper functioning of the skin barrier, as topically applied substances have often to pass the SC lipid regions that form a very dense structure, Therefore, a detailed knowledge about the SC lipid organization is of great importance. The main lipid classes present in the SC are ceramides (CER), cholesterol (CHOL), and free fatty acids (FFA). The ceramide fraction is composed of at least six ceramides, referred to as CER 1, CER 2 . . . CER 6 (1). The FFA and CER both vary in hydrocarbon chain length, the main population of FFA and CER having an acyl chain length between 22 and 26 C atoms.

In diseased skin the barrier function is frequently impaired. There, a deviation in lipid composition has often been found. This includes *i*) a significant change in CER profile in atopic dermatitis and psoriatic scales (2, 3), *ii*) reduced FFA/CHOL and FFA/CER ratios in lamellar ichthyosis patients (4); and *iii*) 3- to 4-fold elevated levels of CSO_4 in recessive X-linked ichthyosis patients (5). It remains to be established whether the impaired barrier function can always be linked to a modulated lipid composition. In order to delineate the link between the barrier function and lipid composition, the role that individual lipid classes play in SC lipid phase behavior should be examined. Such studies with native tissue are hampered

Abbreviations: CHOL, cholesterol; CER, ceramides; FFA, free fatty acids; CSO_4, cholesterol sulfate; λ, wave length; θ, scattering angle; d, periodicity; SC, stratum corneum.

[1] To whom correspondence should be addressed.

by the low availability of the required material from the diseased skin. In order to mimic diseased SC, one can consider to modulate lipid composition in SC isolated from normal skin. However this approach is not feasible, as it is impossible to selectively extract certain lipid classes from the SC. For this reason another approach, like the use of lipid mixtures isolated from SC, should be chosen.

Using X-ray techniques it has been established that in the SC the lipids are organized into two crystalline lamellar phases with periodicities of approximately 6 and 13 nm (6–8). A similar organization has been observed using equimolar mixtures of CHOL, FFA, and CER isolated from pig SC, except that in these mixtures a larger proportion of CHOL appears in separate crystalline domains than observed in SC. These observations have been made in experiments performed at room temperature (9). In this study we have observed that in CHOL:CER mixtures, the phase behavior at room temperature is similar to that of intact SC. However, when the temperature-induced changes in phase behavior were examined, we observed that between 35° and 55°C a new phase with a periodicity varying between 4.3 and 4.5 nm was formed, which remained dominantly present with further increase of the temperature (9). In human SC this phase has not been encountered (8). The presence of such a phase at elevated temperatures indicates a lower stability of the lamellar phases in the lipid mixtures than in the SC. These observations illustrate the relevance for measuring temperature-induced phase changes, as differences in phase behavior at elevated temperature indicate that differences in lipid organization also exist at room temperature. Sometimes this is difficult to trace when performing lipid organization studies only at room temperature.

Not only the major SC lipids, CHOL, CER and FFA, but also minor fractions, like cholesterol sulfate (CSO_4) may affect SC lipid organization. The CSO_4 level throughout the SC does not remain constant, but reaches very low levels in the superficial SC layers (10, 11). In addition, a pH gradient exists in the SC (12–14) and Ca^{2+} also displays a characteristic gradient in the epidermis. Ca^{2+} level increases from the basal layers to the granulosum layer and declines again in the SC (15–17).

One of the methods to investigate the SC lipid organization is X-ray diffraction. However, X-ray diffraction is a bulk method that provides only information on overall lipid organization in the SC and does not allow study of the effects of local changes in pH and CSO_4 and Ca^{2+} contents on lipid organization in native SC. A systematic study can be performed with lipid mixtures prepared from isolated SC lipids. This allows experimental modulation in lipid composition to mimic the situation either at the stratum granulosum(SG)–SC interface (pH 7.4, high Ca^{2+} and high CSO_4 content) or in the superficial SC layers (pH 5–6, low Ca^{2+} and low CSO_4 content). Because a drop in Ca^{2+} concentration already occurs in the lowest SC layers, but CSO_4 content decreases in the most superficial SC layer, the effect of CSO_4 in the absence of Ca^{2+} on the SC lipid organization is also of interest. In our present studies we chose to incorporate either 2% m/m or 10% m/m CSO_4 into equimolar CHOL:CER:FFA mixtures, to approximate the CSO_4 levels observed in normal and in recessive X-linked ichthyosis skin, respectively (5). Furthermore, as substantial amounts of Ca^{2+} are also present in superficial SC layers in psoriatic skin (18) and in skin covered for several weeks by a plaster after bone fracture (M. Ponec, unpublished results), we decided to study also the effect of Ca^{2+} at pH 5. Because at present no information is available on the local Ca^{2+} concentrations in the SC, we have chosen a concentration of 2 mmol Ca^{2+}, similar to that used to study the effect of Ca^{2+} on phospholipid membrane systems (19–23) being used as model systems for cell membranes.

MATERIALS AND METHODS

Isolation of stratum corneum from pig skin

Fresh pig skin was obtained from a slaughter house at the C.D.I. in Lelystad in the Netherlands and SC was isolated from the skin as described before (9).

Extraction, separation, and identification of lipids from stratum corneum

Epidermal lipids were extracted using the method of Bligh and Dyer (24). The extracted lipids were applied on a silicagel 60 (Merck) column with a diameter of 2 cm and a length of 33 cm. The various lipid classes were eluted sequentially using various solvent mixtures as published recently (9). The lipid composition of the collected fractions was established by one-dimensional high performance thin-layer chromatography, as described before (25). For quantification, authentic standards (Sigma) were run in parallel. The quantification was performed after charring using a photodensitometer with automatic peak integration (Desaga, Germany). Isolated CER fractions 1 to 6 were mixed to achieve the same ratio as found in the pig SC.

Preparation of lipid mixtures

The lipids were mixed in various molar ratios, using a mean CER molar weight of 700. For calculation of the mean ceramide molecular weight, the data on the ceramide composition and alkyl chain length distributions (26) were used. Mixtures were prepared from either *i*) CHOL, CER and FFA or *ii*) CHOL, CER, FFA and CSO_4 or *iii*) CHOL, CER, FFA and CSO_4 in the presence of 2 mm $CaCl_2$. For the FFA mixture, we chose long-chain free fatty acids in a molar ratio according to Wertz and Downing (1). The following fatty acids were included in the lipid mixtures: C16:0, C18:0, C22:0, C24:0, and C26:0 in a molar ratio of 1:3:42:37:7, respectively. The mixtures were prepared at either a pH of 7.4, which is the pH close to the stratum corneum–stratum granulosum interface, or a pH 5, which is the pH of the skin surface (9–11). To achieve a pH of 7.4, a HEPES buffer (10 mmol, Na^+ based) was used. To prepare mixtures at a pH of 5, we used a citrate buffer (10 mmol, Na^+ based).

Small angle X-ray diffraction (SAXD)

All measurements were carried out at the Synchrotron Radiation Source at Daresbury Laboratory using station 8.2. The samples were put in a special designed sample holder with two mica windows. A detailed description of the equipment has been given elsewhere (7). The experimental conditions were similar as described before (9). The scattered intensities were measured as a function of θ, the scattering angle. Calibration of the detector was carried out with rattail and cholesterol. From the scattering angle the scattering vector (Q) was calculated $Q = 4\pi(\sin\theta)/\lambda$, in which λ is the wavelength being 0.154 nm at the sample position.

The diffraction pattern of a lamellar is characterized by a series of peaks at equal interpeak distance, $Q_n = n\ Q_1$, in which Q_n is the position of the nth order peak and Q_1 is the position of the 1st order peak. The periodicity can directly be calculated from the position of the peaks $d = n\ 2\ \pi / Q_n$. The diffraction pattern of CHOL is characterized by two peaks at $Q = 1.87$ and $3.74\ nm^{-1}$.

The lipid phase behavior was also measured as a function of temperature. The temperature was increased at a heating rate of 2°C/min between 25° and 95°C. Data collection was carried out continuously. Each minute a new diffraction curve was collected. In such a way each successive set of diffraction data reflects the mean phase behavior during a temperature rise of 2°C.

RESULTS

Phase behavior at room temperature

Mixtures prepared at pH 5. CHOL:CER:FFA mixture. The diffraction pattern of the equimolar CHOL:CER:FFA mix-

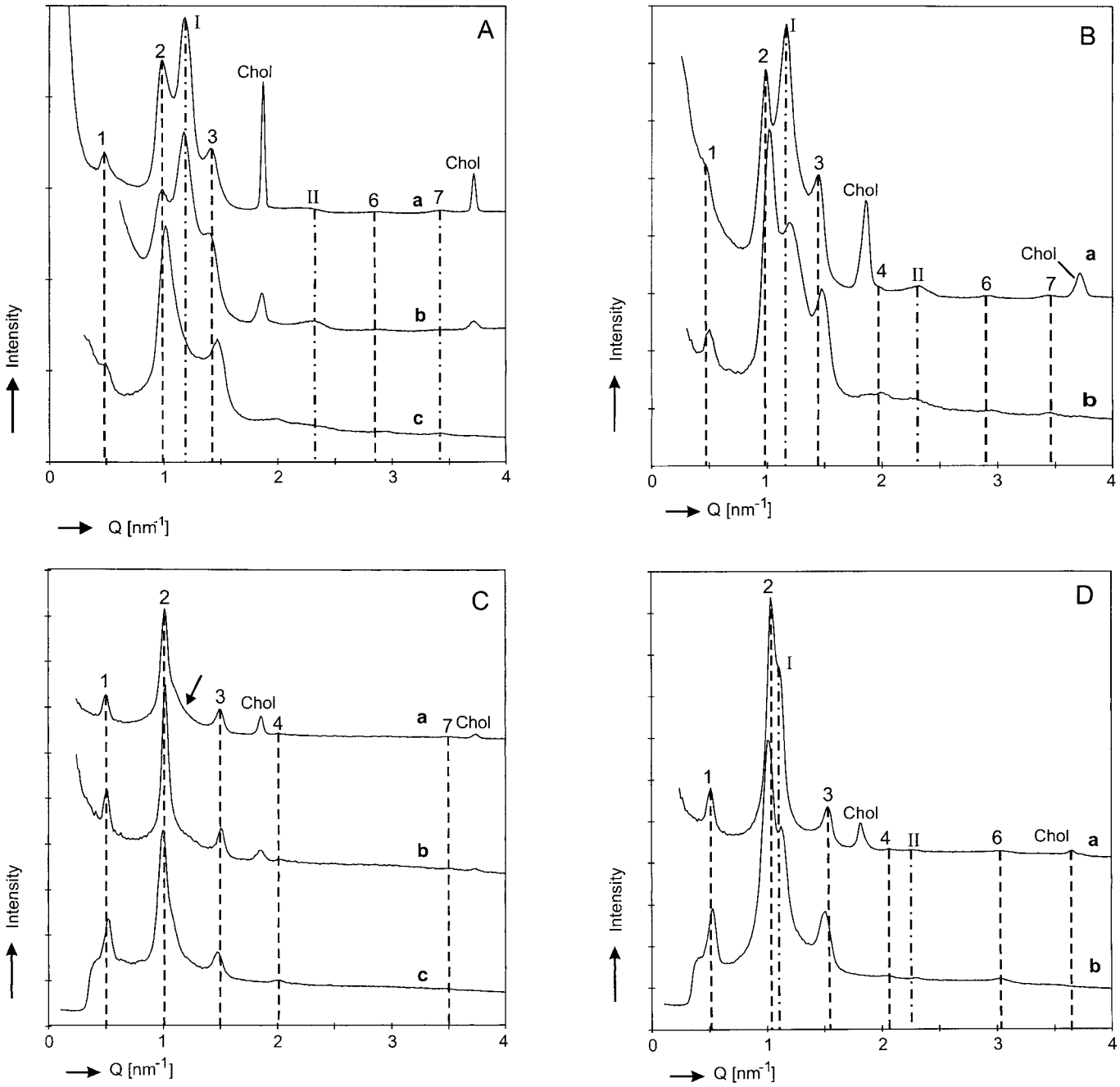

Fig. 1. The effect of CSO_4 and Ca^{2+} on the phase behavior of equimolar CHOL:CER:FFA mixtures. The arabic numbers indicate the diffraction orders of the long periodicity phase (repeat distance between 12 and 13 nm). The roman numbers indicate the diffraction orders of the short periodicity phase (repeat distance between 5.3 and 5.5 nm). The diffraction patterns of the CHOL:CER:FFA:CSO_4 mixtures in molar ratios of A: (a) 1:1:1:0, (b)1:1:1:0.06 and (c) 1:1:1:0.3 at pH 5; B: (a) 1:1:1:0.06 and (b) 1:1:1:0.3 in the presence of 2 mmol Ca^{2+} at pH 5; C: (a) 1:1:1:0, (b) 1:1:1:0.06 and (c) 1:1:1:0.3 at pH 7.4. At curve (a) the shoulder indicated by an arrow refers to the first order diffraction peak of the short periodicity phase; D: (a) 1:1:1:0.06 and (b) 1:1:1:0.3 in the presence of 2 mmol in the presence of 2 mmol Ca^{2+} at pH 7.4.

TABLE 1. Effect of CSO_4 and Ca^{2+} on the lipid organization in equimolar CHOL:CER:FFA mixtures at pH 5

CHOL:CER:FFA (1:1:1)	
13 nm lamellar phase	**1:**[a] 13.0[b](0.48)[c], **2:** 6.4(0.98), **3:** 4.4(1.43), **6:** 2.2(2.85), **7:** 1.84(3.44)
5.4 nm Lamellar phase	**1:** 5.28(1.19), **2:** 2.67(2.34)
CHOL reflection	3.36, 1.69
CHOL:CER:FFA:CSO_4 (1:1:1:0.06)	
12.8 nm lamellar phase	**2:** 6.4(0.98), **3:** 4.48(1.38), **5:** 2.16(2.91)
5.4 nm lamellar phase	**1:** 5.32(1.18), **2:** 2.71(2.32)
CHOL reflections	3.37, 1.69
CHOL:CER:FFA:CSO_4 (1:1:1:0.3)	
12.5 nm lamellar phase	**1:** 12.8(0.49), **2:** 6.17(1.02), **3:** 4.24(1.47), **4:** 3.14(2.00)
CHOL:CER:FFA:CSO_4 (1:1:1:0.06) + Ca^{2+}	
13 nm lamellar phase	**1:** 13(0.49), **2:** 6.4(0.98), **3:** 4.34(1.44), **4:** 3.2(1.96), **6:** 2.14(2.93), **7:**1.82(3.45)
5.4 nm lamellar phase	**1:** 5.4(1.16), **2:** 2.70(2.31)
CHOL reflections	3.37, 1.69
CHOL:CER:FFA:CSO_4 (1:1:1:0.3) + Ca^{2+}	
12.8 nm lamellar phase	**1:** 12.7(0.49), **2:** 6.13(1.02), **3:** 4.25(1.47), **4:** 3.2(1.96), **6:** 2.12(2.95), **7:** 1.82(3.45)
5.4 nm lamellar phase	**1:** 5.22(1.19), **2:** 2.70(2.31)

The repeat distances and corresponding spacings of the lamellar phases and crystalline cholesterol in the lipid mixtures are given.
[a] Order of the reflection in **boldface numbers**.
[b] Spacing corresponding to the reflection in nm.
[c] Q value of the reflection in nm^{-1} (in parentheses). This can be obtained from the corresponding Figs. 1A and 1B.

ture is presented in **Fig. 1A**. The spacings and corresponding periodicities are summarized in **Table 1**. As can be noticed from Table 1 and Fig. 1A, this mixture formed two lamellar phases with periodicities of 13.0 and 5.4 nm, respectively. In addition, 3.36 and 1.69 nm diffraction peaks were observed that could be attributed to CHOL that separates as a phase in crystalline domains. The phase behavior of the equimolar CHOL:CER:FFA mixture was similar to that published recently (9).

CHOL:CER:FFA:CSO_4 mixture. In order to study the effect of CSO_4 on the lipid phase behavior either 2% m/m or 10% m/m CSO_4 has been incorporated into the equimolar CHOL:CER:FFA mixture. Inspection of Table 1 and Fig. 1A revealed that lipids in CHOL:CER:FFA:CSO_4 mixture in a molar ratio of 1:1:1:0.06 (2% m/m) formed two lamellar phases with periodicities of 12.8 and 5.4 nm, respectively, similar to that seen in the absence of CSO_4. Furthermore, the intensity of peaks attributed to crystalline CHOL decreased. A further increase in CSO_4 content to 10% m/m (molar ratio:1:1:1:0.3) induced a pronounced change in the lamellar phase behavior: the diffraction peaks attributed to the 5.4 nm phase and the peaks assigned to crystalline CHOL disappeared (Fig. 1A).

CHOL:CER:FFA:CSO_4 and Ca^{2+}. The diffraction curve and corresponding spacings are depicted in Fig. 1B and Table 1, respectively. Addition of 2 mmol $CaCl_2$ to a CHOL:CER:FFA:CSO_4 mixture in a molar ratio of 1:1:1:0.06 did not affect the peak intensities attributed to the 5.4 and 13.0 nm lamellar phases, but slightly increased the intensity of the CHOL reflections. This indicates that at low CSO_4 the presence of Ca^{2+} decreased the CHOL solubility in the lamellar phases. In contrast to that, addition of Ca^{2+} to 1:1:1:0.3 CHOL:CER:FFA:CSO_4 mixture did not result in the reappearance of the CHOL reflections. However, a reappearance of the 5.4 nm peak was observed.

The results at pH 5 demonstrate that CSO_4 increases the solubility of CHOL in the lamellar phases and when present at high levels it promotes the formation of the long periodicity phase, while Ca^{2+} counterbalances partly the lipid phase changes induced by CSO_4.

Mixtures prepared at pH 7.4. CHOL:CER:FFA mixtures. The phase behavior of the equimolar CHOL:CER:FFA mixtures prepared at a pH of 7.4 is shown in Fig. 1C and the corresponding spacings are presented in **Table 2**. From Fig. 1C and Table 2 it is obvious that at pH 7.4 only one dominant lamellar phase was present, with a periodicity of 12.6 nm, which is in good agreement with our recent findings (27). The 6.2 nm peak (2nd order peak of the 12.5 nm phase) was asymmetric with a shoulder on its right-hand side, indicating the presence of an additional peak at a slightly shorter spacing (see arrow in Fig. 1C). This shoulder is most likely the first order diffraction peak of the 5–6 nm phase, which is prominently present at a pH 5 (see above). In addition, two diffraction peaks at 3.37 and 1.68 nm were observed that could be attributed to crystalline cholesterol.

CHOL:CER:FFA:CSO_4 mixture. Incorporation of 2% m/m CSO_4 into the equimolar CHOL:CER:FFA mixture caused a change of the 6.2 nm asymmetric peak into a symmetric one (2nd order peak of the 12.4 nm phase) and a slight reduction of the intensities of the CHOL reflections (Fig. 1B). From these observations it is obvious that in the presence of 2% m/m CSO_4 the formation of the 5–6 nm phase was suppressed and the solubility of CHOL in the lamellar phases was increased. An increase in CSO_4 content to 10% m/m increased the solubility of CHOL further. No further changes in the 12.5 nm lamellar phase were observed.

CHOL:CER:FFA:CSO_4 and Ca^{2+}. As shown in Table 2 and Fig. 1D, addition of 2 mm Ca^{2+} to the 1:1:1:0.06 mixture of CHOL:CER:FFA:CSO_4 induced a reappearance of a 5.4 nm shoulder at the right-hand side of the 6.2 nm diffraction peak. Furthermore, in the presence of Ca^{2+}, the intensities of the peaks attributed to crystalline CHOL

TABLE 2. Effect of CSO_4 and Ca^{2+} on the lipid organization in equimolar CHOL:CER:FFA mixtures at pH 7.4

CHOL:CER:FFA (1:1:1)	
12.6 nm lamellar phase	**1:**[a] 12.5[b](0.50)[c], **2:** 6.2(1.02), **3:** 4.18(1.50), **4:** 2.2(2.00), **7:** 1.80(3.49)
5–6 nm lamellar phase	shoulder at 6.2 nm peak
CHOL reflections	3.37, 1.68
CHOL:CER:FFA:CSO_4 (1:1:1:0.06)	
12.4 nm lamellar phase	**1:** 12.4(0.51), **2:** 6.2(1.02), **3:** 4.17(1.50),
CHOL reflections	3.37, 1.69
CHOL:CER:FFA:CSO_4 (1:1:1:0.3)	
12.5 nm lamellar phase	**1:** 12.1(0.52), **2:** 6.3(1.00), **3:** 4.24(1.47), **4:** 3.13(2.00)
CHOL:CER:FFA:CSO_4 (1:1:1:0.06) + Ca^{2+}	
12.3 nm lamellar phase	**1:** 12.3(0.51), **2:** 6.1(1.03), **3:** 4.11(1.53), **4:** 3.04(2.07), **6:** 2.08(3.01),
5.4 nm lamellar phase	**1:** 5.5(1.14, shoulder), **2:** 2.70(2.32)
CHOL reflections	3.37, 1.69
CHOL:CER:FFA:CSO_4 (1:1:1:0.3) + Ca^{2+}	
12.4 nm lamellar phase	**1:** 12.0(0.48), **2:** 6.2(1.01), **3:** 4.16(1.51), **4:** 3.08(2.07), **6:** 2.07(3.01)
5.4 nm lamellar phase	**1:** 5.5(1.15, shoulder), **2:** 2.70(2.32)

The repeat distances and corresponding spacings of the lamellar phases and crystalline cholesterol in the lipid mixtures at pH 7.4 are given.
[a] Order of the reflection in **boldface numbers**.
[b] Spacing corresponding to the reflection in nm.
[c] Q value of the reflection in nm^{-1} (in parentheses). This can be obtained from the corresponding Figs. 1C and 1D.

increased. Addition of Ca^{2+} to the 1:1:1:0.3 mixture of CHOL:CER:FFA:CSO_4 also caused a reappearance of the 5.4 nm shoulder, but no CHOL reflections were observed. The above results indicate that 2 mmol Ca^{2+} balances, at least partly, the changes in lipid phase behavior induced by CSO_4.

The results at pH 7.4 obviously show that CSO_4 increases the solubility of CHOL and promotes the formation of the long periodicity phase, while Ca^{2+} opposes the effect similar to that observed at pH 5.

Temperature-induced changes in the SC lipid phase behavior of mixtures prepared at pH 5

CHOL:CER:FFA mixtures. The phase behavior of the CHOL:CER:FFA mixtures has been followed as a function of temperature between 25° and 95°C (**Fig. 2A**). Each curve represents the lipid phase behavior during a 2°C rise in temperature. The phase behavior at room temperature is similar to that shown in Fig. 1A. Two lamellar phases are present with periodicities 13.0 and 5.4 nm, respectively. The peaks attributed to the 5.4 and 13.0 nm phases start to decrease in intensity at approximately 55°C and disappear at about 63°C. At approximately 35–39°C a new 4.3 nm peak is formed. A further temperature rise leads to a strong increase in the intensity of this peak and to a small shift in position to a spacing of 4.4 nm. Simultaneously with the increase in intensity of the 4.3 nm peak between 39° and 63°C, a 2.2 nm peak appears. This peak can most likely be attributed to the same phase, as it follows the positional and intensity changes of the 4.4 nm peak. At around 60°C the 4.4 nm peak transforms into a doublet that turns to a singlet again at 71°C. A further increase in temperature reduces the 4.4 nm and 2.2 nm peak intensity, but at 95°C the reflections are still present. The CHOL reflections start to decrease in intensity at approximately 37°C and disappear at around 55°C.

CHOL:CER:FFA:CSO_4 mixture. As depicted in Fig. 2B, no changes in the lipid phase behavior have been noticed in the 1:1:1:0.06 CHOL:CER:FFA:CSO_4 mixture until the temperature reaches approximately 45°C. Between 50° and 55°C the CHOL diffraction peaks gradually reduced in intensity and subsequently disappeared at about 55°C. At about 60°C the intensity of the diffraction peaks attributed to the 5.4 and 12.8 nm lamellar phases started to decrease. In contrast to the observations made with the CHOL:CER:FFA mixture, no new 4.3 nm peak appeared at 35–39°C, but the intensity of the 4.4 nm diffraction peak (3rd order of the 12.8 nm lamellar phase) started to increase at around 45°C. It is not clear whether in this temperature region it is caused by the formation of a new phase with a peak position at exactly the same spacing as the already existing peak or that the intensity increase is caused by a change in the lipid organization of the 12.8 nm phase. A further rise in temperature caused a further increase in the 4.4 nm peak intensity. A maximum peak intensity was reached at 61°C. The observation that the diffraction peaks attributed to the 5.4 and 12.8 nm phases disappear at 65°, while the 4.4 nm phase was still present, is indicative for the formation of a new 4.3 nm phase. The 4.4 nm peak disappeared at approximately 83°C.

As depicted in Fig. 2C, the presence of 2 mmol Ca^{2+} had a profound effect on the phase behavior of the 1:1:1:0.06 CHOL:CER:FFA:CSO_4 mixtures at elevated temperature. Most substantial is the increase in 4.4 nm peak intensity that starts already at around 40°C. A further increase in temperature increased the peak spacing and peak intensity gradually. The peak intensity reached its maximum at approximately 67°C. Above this temperature the peak intensity and spacing decreased. At 95°C the peak (4.2 nm spacing) was still present. Because the 5.4 and 13 nm phases disappeared at 70°C, it is obvious that a new phase appeared at high temperature with a 2nd order peak at 2.15 nm (see arrow).

Our studies reveal that the presence of CSO_4 is required to mimic SC lipid phase behavior over a wide temperature range and that Ca^{2+} acts partly towards the

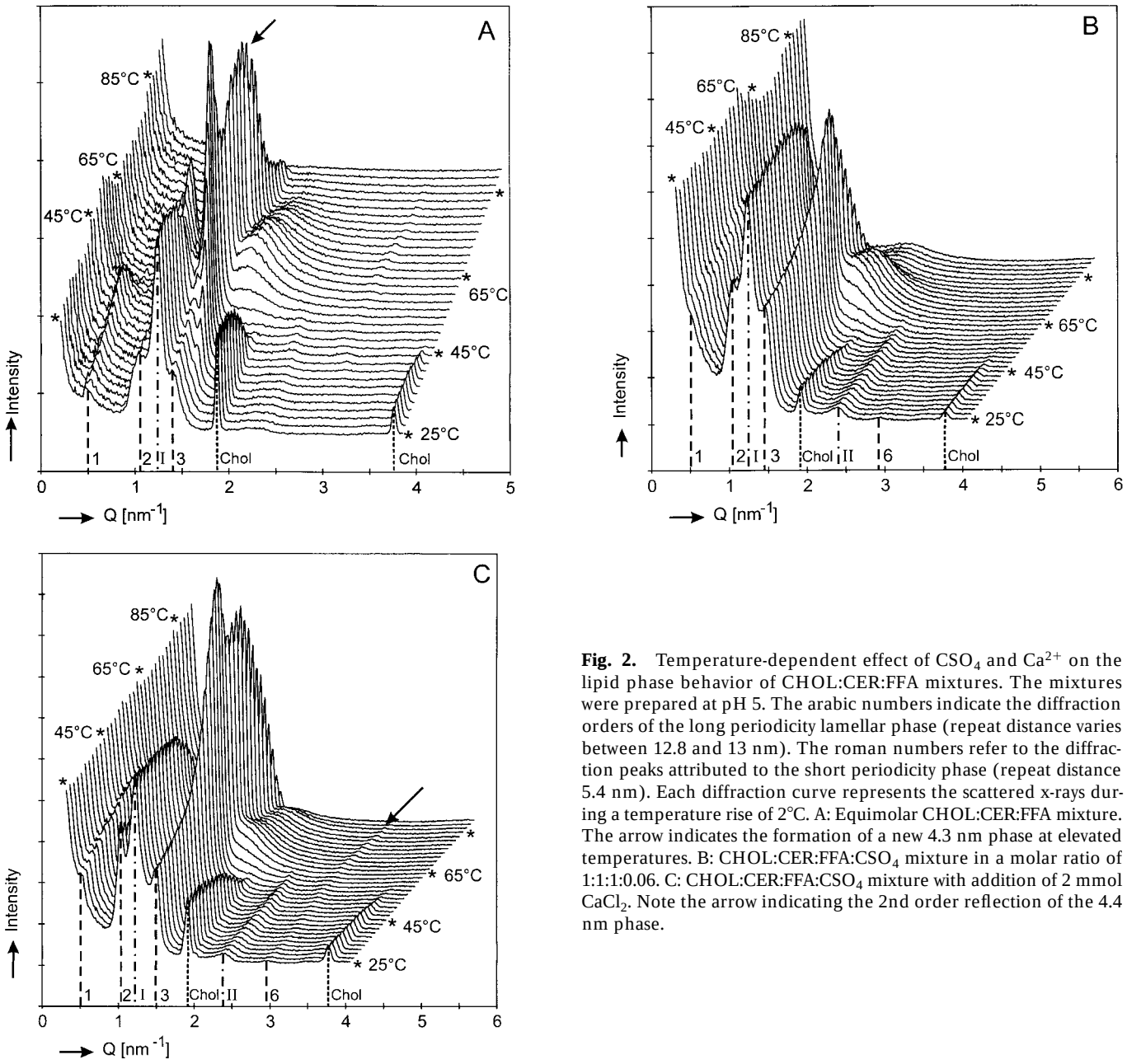

Fig. 2. Temperature-dependent effect of CSO_4 and Ca^{2+} on the lipid phase behavior of CHOL:CER:FFA mixtures. The mixtures were prepared at pH 5. The arabic numbers indicate the diffraction orders of the long periodicity lamellar phase (repeat distance varies between 12.8 and 13 nm). The roman numbers refer to the diffraction peaks attributed to the short periodicity phase (repeat distance 5.4 nm). Each diffraction curve represents the scattered x-rays during a temperature rise of 2°C. A: Equimolar CHOL:CER:FFA mixture. The arrow indicates the formation of a new 4.3 nm phase at elevated temperatures. B: CHOL:CER:FFA:CSO_4 mixture in a molar ratio of 1:1:1:0.06. C: CHOL:CER:FFA:CSO_4 mixture with addition of 2 mmol $CaCl_2$. Note the arrow indicating the 2nd order reflection of the 4.4 nm phase.

CSO_4 effect not only at room temperature, but also at elevated temperatures.

DISCUSSION

During epidermal differentiation, characteristic changes in lipid composition occur, consistent with the formation of a waterproof barrier. These changes include a progressive depletion of phospholipids and glucosphingolipids accompanied by enrichment in CER, CHOL, FFA, and small amounts of other polar (e.g., CSO_4) and nonpolar lipid species (cholesteryl esters and triglycerides). The relative amounts of CHOL, CER and FFA remain unchanged throughout the whole SC (M. Ponec and A. Weerheim, unpublished results). There is increasing evidence that within the SC also no significant change in CER composition occurs (28).

The SC intercellular lipid bilayers originate from lamellar bodies that are abundantly present in the SG and are extruded to intercellular space at the SG/SC interface. After extrusion, the content of lamellar bodies is reorganized into lamellae. It has been suggested that the presence of Ca^{2+} is required for the formation of intercellular lamellae (29). The Ca^{2+} concentration is high at the SG/SC interface and in the first SC layers. Subsequently, it drops to very low levels in the upper SC. Not only the Ca^{2+} levels but also the pH and CSO_4 content decrease in the direction of the skin surface (11–14, 30, 31).

The previous (27) and present studies have shown that the solubility of cholesterol in equimolar CHOL:CER:FFA mixtures increases in the presence of CSO_4 (**Fig. 3**). Most likely the increased solubility of CHOL in the lamellar phases can be ascribed to the presence of the charged sul-

fate group. Due to the electric repulsion forces, the charged sulfate group increases the interfacial area per lipid molecule and thus reduces the lattice density and/or increases the chain mobility in the bilayers. This is in agreement with our recent findings (27) which showed that in the absence of CSO_4 the CHOL:CER:FFA mixtures form an orthorhombic phase, while upon addition of CSO_4 a liquid lateral packing appears. An increased fluidity has indeed been found in recessive X-linked ichthyosis by electron spin resonance (32). Studies of Kitson et al. (33) revealed that intercalation of CSO_4 in sphingomyelin bilayers increased the transition temperature of the lamellar to reversed hexagonal phase. They explained this phenomenon by an increase in the interfacial area. A stabilization of the membrane structure by CSO_4 has also been found in other phospholipid systems (21, 34).

The formation of the long periodicity phase is also promoted by an increase in pH from 5 to 7.4. This pH change also increases the repulsion forces between the lipids and therefore is expected to reduce the lattice density and increase the chain mobility as well. These observations suggest a more general mechanism, namely that a reduction in lattice density or an increase in chain mobility promotes the formation of the 12–13 nm phase. This hypothesis is supported by at least two other recent observations. In SC isolated from reconstructed human epidermis and from murine skin, lattice density is reduced: in the former a hexagonal lateral packing is present (35), while in the latter a liquid phase coexists with an orthorhombic lateral packing (6). In both SC samples the 12–13 nm lamellar phase dominates.

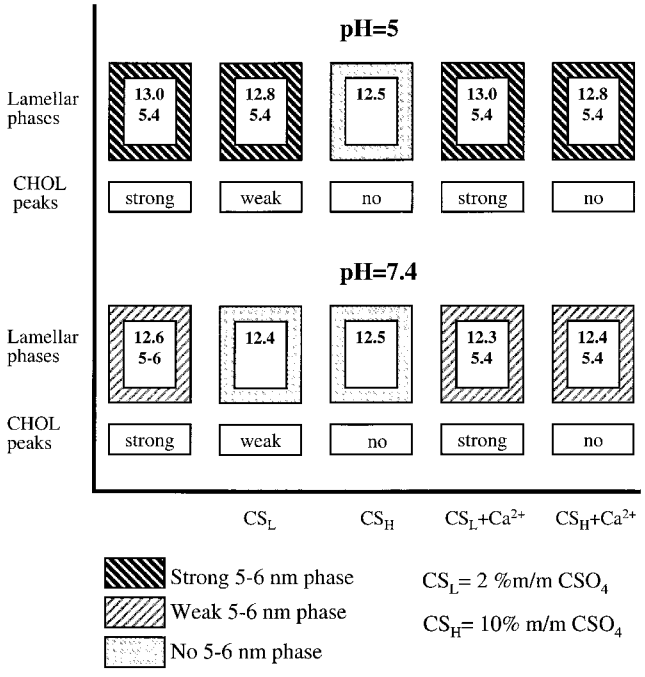

Fig. 3. A schematic presentation of the changes in the lipid phase behavior in equimolar CHOL:CER:FFA mixtures by changes of pH, Ca^{2+} (2 mmol), and CSO_4 content. The long periodicity phase, repeat distance of which varied between 12.4 and 13 nm, was always prominently present. The intensity of the 1st order diffraction peak attributed to the short periodicity phase (repeat distance varied between 5 and 6) varied strongly. This peak, indicative for the presence of the short periodicity phase, has been categorized in the following way: strong, weak and not present.

It has often been suggested that CSO_4 plays an important role in the desquamation process. Recently it has been shown that CSO_4 inhibits the enzymatic activity of enzymes responsible for desmosomal degradation (36). A drop in the CSO_4 content in the superficial SC layers (10, 11) will activate these enzymes and facilitate the desquamation process. However, not only the desmosomes, but also the lipid bilayers are responsible for the intercellular cohesion in the SC. The results of the present study demonstrate that a drop in the CSO_4 content will affect the SC lipid phase behavior. As observed from the measurements at elevated temperature (see below), the reduction in CSO_4 content decreases the stability of the bilayers and reduces the fraction of lipids arranged in a liquid lateral packing (27). The absence of this fluid phase is expected to reduce the elasticity of the lipid phases (37) and might even prevent the lamellae from following the contours of the corneocyte surfaces. This will decrease the cohesion between the cells and promote the desquamation process. Therefore, our data suggest that CSO_4 plays an important role in a proper functioning of the SC. In deeper SC layers CSO_4 increases the lipid mobility and, in the superficial layers, the decrease in CSO_4 levels promotes the desquamation process not only due to the increased desmosomal degradation (36), but also by destabilizing the lipid lamellar phases.

Changes induced by CSO_4 can be partly counterbalanced by the presence of 2 mmol Ca^{2+} (Fig. 3). Namely, while 2% CSO_4 increases the solubility of CHOL in the lamellar phases, Ca^{2+} promotes formation of separate crystalline CHOL domains in the presence of 2% m/m CSO_4. Furthermore, while the 5–6 nm reflection at pH 7.4 disappears in the presence of 2 or 10% m/m CSO_4, in the presence of Ca^{2+} reappearance of the 5–6 nm reflection occurs. At pH 5 the same events are observed with 10% m/m CSO_4. These findings indicate that in the presence of 2 mmol Ca^{2+} the formation of the 5–6 nm phase and the reformation of crystalline domains of CHOL is facilitated. However, in mixtures containing 10% m/m CSO_4, most probably the CSO_4 content is increased to such high levels that the formation of CHOL crystals is prevented. In phospholipid systems Ca^{2+} stimulates dehydration of phospholipid head groups and induces crystallization. This has been demonstrated for cardiolipin, phosphatidylserine, phosphatidylglycerol, and phosphatidylcholine (19–23). Because hardly any water is present between the bilayers in CER:CHOL:FFA mixtures it is unlikely that a similar mechanism is involved. Most likely Ca^{2+} is able to reduce the surface charge density induced by either CSO_4 or dissociated FFA (the pKa values of the fatty acids are approximately 6–6.5 (38). This results in a reduction of the intermolecular electrostatic repulsion and an increase in lattice density. Whether Ca^{2+} links two opposing CSO_4 lipids as suggested in a previous paper (32) remains to be established. Consequently, when extrapolating these

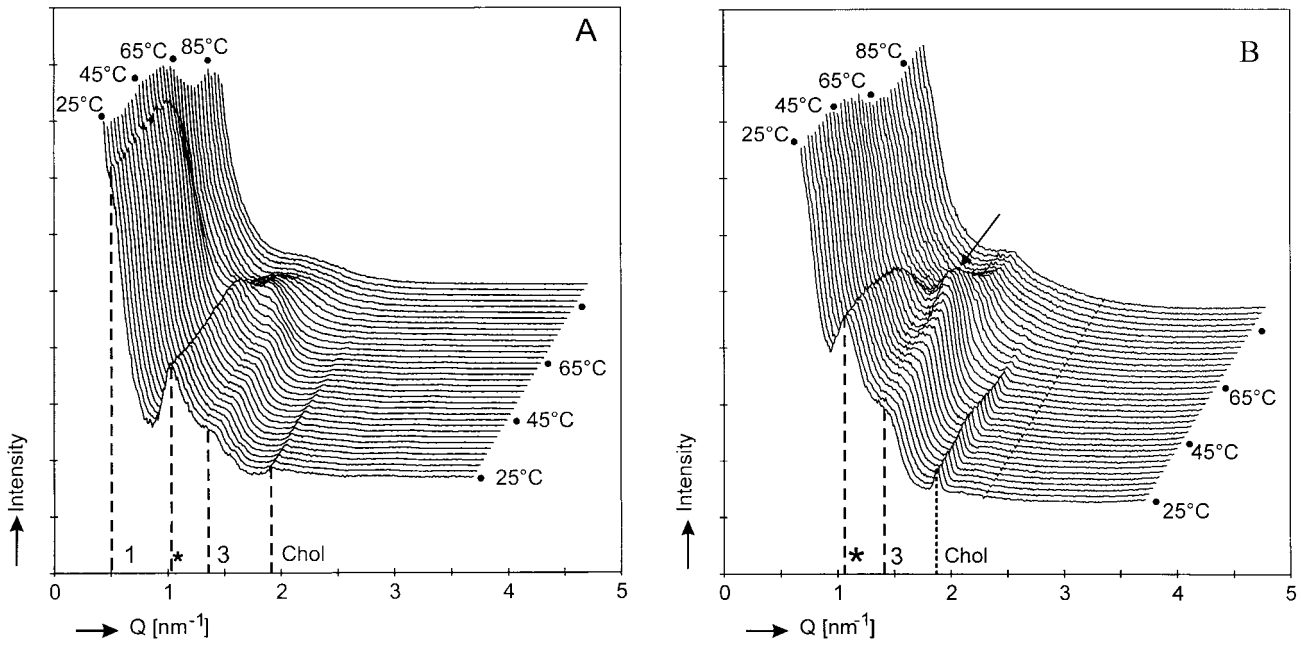

Fig. 4. Temperature-induced changes in the diffraction pattern of pig and human SC. The arabic numbers indicate the diffraction orders of the 13 nm lamellar phase. The peak indicated by an asterisk is attributed to the 2nd order diffraction peak of the 13 nm phase and the 1st order of the 6 nm phase. Each diffraction curve represents the scattered X-rays during a temperature rise of 2°C. A: Human stratum corneum. Note the appearance of a new phase at around 50°C (see arrow). B: Pig stratum corneum. No new phase has been formed at elevated temperatures.

findings to the situation in intact SC, changes induced by CSO_4 might be partly counterbalanced by Ca^{2+}. In normal skin this occurs only in the lowest SC layers where Ca^{2+} is present. In higher SC layers no Ca^{2+} could be detected (17). In contrast to this, CSO_4 levels remain unchanged up to the superficial SC cell layers. The observation that in about 50% of the human SC samples a small amount of CHOL phase separates (J. A. Bouwstra, G. S. Gooris, A. Weerheim, and M. Ponec, unpublished results) indicates that the level of CSO_4 is probably such that the SC lamellae are partially or completely saturated with CHOL. At the most superficial SC layer the CSO_4 level drops, which might induce a crystallization of CHOL and decrease the cohesion between the lipid lamellae.

At 10% m/m CSO_4 levels, only the 12–13 nm phase is present. One can expect that in recessive x-linked ichthyosis skin, in which the CSO_4 level is increased from 3.4% w/w to 11.2% w/w (5), a change in the lipid phase behavior occurs. In a previous study (27) it has been shown that at low CSO_4 levels a fraction of lipids is arranged in a liquid lateral packing. One can speculate that a further increase in CSO_4 levels, as observed in recessive x-linked ichthyosis SC, might reduce the lattice density further and consequently might increase the permeability of the SC, which is in agreement with previous findings (32). The consequences of the presence of only the 12–13 nm phase for the skin barrier function is yet unknown.

Phase behavior at elevated temperatures

Although it has been observed that at room temperature the CHOL:CER and CHOL:CER:FFA mixtures mimic the SC lipid organization quite closely, one may conclude that the phase behavior of the mixtures is similar to that in the SC only when the phase behavior of the lipid mixtures resembles that of SC over a wide temperature range. Furthermore, it has often been demonstrated that the lipid phase behavior is more sensitive to compositional changes at increased temperature than at room temperature (39). In a previous paper (9) we have reported that at increased temperature an additional phase, indicated by 4.3 nm spacing, is formed in CHOL:CER mixtures, which is more prominently present when the temperature is increased. This 4.3 nm phase has hardly ever been observed in SC derived from healthy persons and is only weakly present in pig SC (**Fig. 4A and B**), but it has been observed in a pilot study in psoriatic scales (J. A. Bouwstra, unpublished results). From the experiments presented here it became clear that in the presence of only 2% m/m CSO_4 the appearance of the 4.3 nm phase shifts to higher temperatures and that the intensity of the corresponding diffraction peak reduces remarkably. This finding demonstrates that the SC lipid phase behavior is mimicked more closely in the presence of CSO_4 than in its absence. In addition, the 5.4 and 12.8 nm lamellar phases remain stable over a larger temperature range and the phases are less sensitive for temperature-induced changes. This clearly indicates that CSO_4 increases the stability of these phases. The situation is different when Ca^{2+} is also present. There the intensity of the 4.4 nm peak starts to increase at lower temperature, indicating that Ca^{2+} destabilizes the lamellar phases and counteracts the effect of CSO_4. Therefore an increase in Ca^{2+} level, such as present in psoriatic

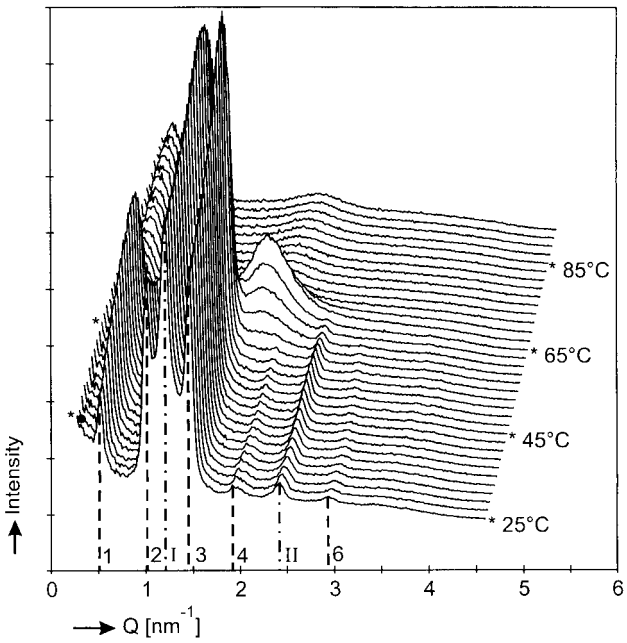

Fig. 5. Temperature-induced changes in diffraction patterns of the CHOL:CER:FFA mixture prepared in a molar ratio of 0.6:1:1 at pH 5. Each curve represents the phase behavior during a temperature rise of 2°C. The arabic numbers indicate the diffraction orders of the 12.8 nm. The roman numbers indicate the diffraction orders of the 5.4 nm lamellar phase.

scales (18), might lead to destabilization of the SC lipid organization.

To elucidate whether the stabilization of the lamellar phases by CSO_4 is caused by the introduction of the negative charge in the lamellae or whether it is due to the increased solubility of CHOL, we performed an additional experiment in which the CHOL content in CHOL:CER:FFA mixture (pH = 5) was reduced to such a level that no crystalline CHOL was present. In the 0.6:1:1 CHOL:CER:FFA mixture no separated crystalline domains of CHOL were detected, see **Fig. 5** and increase in temperature up to 60°C did not affect the lipid phase behavior. At this temperature the diffraction peaks attributed to the 5.4 and 12.8 nm phases start to reduce in intensity and finally disappear between 60° and 70°C. In the same temperature region, a very broad diffraction peak is observed that disappears at approximately 75°C. No increase in the intensity of the 4.4 nm peak has been observed in this mixture. When extrapolating these results to 1:1:1:0.06 CHOL:CER:FFA:CSO_4 mixture, it became clear that in the diffraction pattern of this mixture the reduction in the 4.4 nm peak intensity at elevated temperatures is not caused by the presence of an additional negative charge introduced by CSO_4, but can be ascribed to the decrease in crystalline CHOL that separates as a phase at room temperature. This obviously demonstrates that the increased stability of the lamellar phases induced by CSO_4 is based on its capacity to enhance the solubility of CHOL in the lamellar phases.

In conclusion, despite a low CSO_4 level present in SC of normal skin, CSO_4 might be important in stabilizing the lamellar phases in the deeper layers of the SC. Furthermore, its absence in the superficial layers of SC might destabilize the lipid lamellae and therefore facilitate the desquamation process.

Manuscript received 24 May 1999 and in revised form 31 August 1999.

REFERENCES

1. Wertz, P. W., and D. T. Downing. 1991. Epidermal lipids. *In* Physiology, Biochemistry and Molecular Biology in the Skin. 2nd Edition. L. A. Goldsmith, editor. Oxford University Press, Oxford. 205–236.
2. Motta, S., M. Monti, S. Sesana, L. Mellesi, R. Ghidoni, and R. Caputo. 1994. Abnormality of water barrier function in psoriasis. *Arch. Dermatol.* **13:** 452–456.
3. Motta, S., M. Monti, S. Sesana, L. Mellesi, R. Caputo, S. Carelli, and R. Ghidoni. 1993. Ceramide composition of the psoriatic scale. *Biochim. Biophys. Acta.* **1182:** 147–151.
4. Lavrijsen, A. P. M., J. A. Bouwstra, G. S. Gooris, H. E. Boddé, and M. Ponec. 1995. Reduced skin barrier function parallels abnormal stratum corneum lipid organisation in patients with lamellar ichthyosis. *J. Invest. Dermatol.* **105:** 619–624.
5. Elias, P. M., M. L. Williams, M. E. Maloney, J. A. Bonifas, B. E. Brown, S. Grayson, and E. H. Epstein. 1984. Stratum corneum lipids in disorders of cornification. *J. Clin. Invest.* **74:** 1414–1421.
6. White, S. H., D. Mirejovsky, and G. I. King. 1988. Structure of lamellar lipid domains and corneocytes envelopes of murine stratum corneum. An X-ray diffraction study. *Biochemistry.* **27:** 3725–3732.
7. Bouwstra, J. A., G. S. Gooris, J. A. van der Spek, and W. Bras. 1991. The structure of human stratum corneum as determined by small angle X-ray scattering. *J. Invest. Dermatol.* **96:** 1006–1014.
8. Bouwstra, J. A., G. S. Gooris, W. Bras, and D. T. Downing. 1995. Lipid organization in pig stratum corneum. *J. Lipid Res.* **36:** 685–695.
9. Bouwstra, J. A., G. S. Gooris, K. Cheng, A. Weerheim, W. Bras, and M. Ponec. 1996. Phase behavior of isolated skin lipids. *J. Lipid Res.* **37:** 999–1011.
10. Cox, P., and C. A. Squier. 1986. Variations in lipids in different layers of porcine epidermis. *J. Invest. Dermatol.* **87:** 741–744.
11. Ranasinghi, A., P. W. Wertz, D. T. Downing, and I. C. Mackenzie. 1986. Lipid composition of cohesive and desquamated corneocytes from mouse ear skin. *J. Invest. Dermatol.* **86:** 187–190.
12. Aly, R., C. Shirley, B. Cumico, and H. I. Maibach. 1978. Effect of prolonged occlusion on the microbial flora, pH, carbon dioxide and transepidermal water loss on human skin. *J. Invest. Dermatol.* **71:** 378–381.
13. Turner, N., C. Cullander, and R. H. Guy. 1998. Determination of the pH gradient across the stratum corneum. *J. Invest. Dermatol. Symp. Proceed.* **3:** 110–113.
14. Sage, B. H., R. H. Huke, A. C. Mc Farland, and K. Kowalczyk. 1993. The importance of skin pH in iontophoresis of peptides. *In* Prediction Percutaneous Penetration. K. Brain, V. James, and K. A. Walters, editors. STS Publishing, Cardiff. 410–418.
15. Menon, G. K., J. Grayson, and P. M. Elias. 1985. Ion calcium reservoirs in mammalian epidermis: ultrastructural localization by ion-capture cytochemistry. *J. Invest. Dermatol.* **84:** 508–512.
16. Forslind, B. 1987. Quantitative X-ray microanalysis of skin. *Acta Derma Venerol. (Suppl.)* **134:** 1–8.
17. Vicanová, J., E. Boelsma, A. M. Mommaas, J. A. Kempenaar, B. Forslind, J. Pallon, T. Egelrud, H. K. Koerten, and M. Ponec. 1998. Normalized epidermal calcium distribution profile in reconstructed epidermis is related to improvement of terminal differentiation and stratum corneum barrier formation. *J. Invest. Dermatol.* **97:** 97–106.
18. Menon, G. K., and P. M. Elias. 1991. Ultrastructural localization of calcium in psoriatic and normal human epidermis. *Arch Dermatol.* **127:** 57–63.
19. Papahadjopoulus, D., W. J. Vail, C. Newton, S. Nir, K. Jacobson, G. Poste, and R. Lazo. 1977. Studies on membrane fusion. III. The role of calcium-induced phase changes. *Biochim. Biophys. Acta.* **465:** 579–598.
20. Hope, M. J., and P. Cullis. 1980. Effects of divalent cations and pH on phosphatidylserine model membranes: a ^{31}P NMR study. Biochem. Biophys. Res. Commun. **92:** 846–852.

21. Cheetham, J. J., R. J. Chen, and R. M. Epand. 1990. Interaction of calcium and cholesterol sulphate induces membrane destabilization and fusion: implications for the acrosome reaction. *Biochim. Biophys. Acta.* **1024:** 367–372.
22. Killian, J. A., M. C. Koorengevel, J. A. Bouwstra, G. S. Gooris, W. Dowhan, and B. de Kruijff. 1994. Effect of divalent cations on lipid organisation of cardiolipin isolated from *Escherichia coli* strain AH930. *Biochim. Biophys. Acta.* **1189:** 225–232.
23. Smaal, E. B., K. Nicolay., J. Mandersloot, B. De Kruijff, and J. De Gier. 1987. Calcium-induced changes in permeability of dioleoylphosphatidylcholine model membranes containing bovine heart cardiolipin. *Biochim. Biophys. Acta.* **897:** 191–196.
24. Bligh, E. G., and W. J. Dyer. 1959. A rapid method of total lipid extraction and purification. *Can. J. Biochem. Physiol.* **37:** 911–917.
25. Ponec, M., A. Weerheim, J. Kempenaar, A. M. Mommaas, and D. H. Nugteren. 1988. Lipid composition of cultured human keratinocytes in relation to their differentiation. *J. Lipid Res.* **29:** 949–962.
26. Wertz, P. W., and D. T. Downing. 1983. Ceramides of pig stratum epidermis, structure determination. *J. Lipid Res.* **24:** 753–758.
27. Bouwstra, J. A., G. S. Gooris, F. E. R. Dubbelaar, A. Weerheim, and M. Ponec. 1998. pH, cholesterol sufate and fatty acids affect stratum corneum lipid organisation. *J. Invest. Dermatol. Proceedings* **3:** 69–74.
28. Lavrijsen, A. P. M., I. M. Higounenc, A. Weerheim, E. Oestmann, E. E. Tuinenburg, H. E. Boddé, and M. Ponec. 1994. Validation of an in vivo extraction method for human stratum corneum ceramides. *Arch. Dermatol. Res.* **286:** 495–503.
29. Abraham, W., P. W. Wertz, L. Landmann, and D. T. Downing. 1987. Stratum corneum lipid liposomes: calcium-induced transformation into lamellar sheets. *J. Invest. Dermatol.* **88:** 212–214.
30. Ohman, H., and A. Vahlquist. 1994. In vivo studies concerning a pH gradient in human stratum corneum and upper epidermis. *Acta. Derm. Venereol.* **74:** 375–379.
31. Ohman, H., and A. Vahlquist. 1998. The pH gradient over the stratum corneum differs in X-linked recessive and autosomal dominant ichthyosis: a clue to the molecular origin of the "acid skin mantle"? *J. Invest. Dermatol.* **111:** 674–677.
32. Rehfeld, S. J., W. Z. Plachy, M. L. Williams, and P. M. Elias. 1988. Calorimetric and electron spin resonance examination of lipid phase transitions in human stratum corneum: molecular basis for normal cohesion and abnormal desquamation in recessive X-linked ichthyosis. *J. Invest. Dermatol.* **91:** 499–505.
33. Kitson, N., M. Monck, J. Thewalt, and P. Cullis. 1992. The influence of CSO_4 on phase behavior and hydrocarbon order in model membranes. *Biochim. Biophys. Acta.* **1111:** 127–133.
34. Epand, R. M., R. Bottega, and K. Robinson. 1990. Cholesteryl phosphate and cholesteryl pyrophosphate inhibit formation of the hexagonal phase. *Chem. Phys. Lipids.* **55:** 49–53.
35. Bouwstra, J. A., G. S. Gooris, A. Weerheim, J. A. Kempenaar, and M. Ponec. 1995. Characterization of stratum corneum structure in reconstructed epidermis by X-ray diffraction. *J. Lipid Res.* **36:** 496–504.
36. Sato, J., M. Denda, J. Nakanishi, J. Nomura, and J. Koyama. 1998. Cholesterol sulfate inhibits proteases that are involved in desquamation of stratum corneum. *J. Invest. Dermatol.* **111:** 189–93.
37. Forslind, B. 1994. A domain mosaic model of the skin barrier. *Acta Derm. Venereol.* **74:** 1–6.
38. Lieckfeldt, R., J. Villalain, J-C. Gómez-Fernández, and G. Lee. 1996. Apparant pKa of the fatty acids within ordered mixtures of model human stratum corneum lipids. *Pharm. Res.* **12:** 1614–1617.
39. Sheddon, J. M. 1990. Structure of inverted hexagonal(H_{II}) phase, and non-lamellar phase transitions of lipids. *Biochim. Biophys. Acta.* **1031:** 1–69.